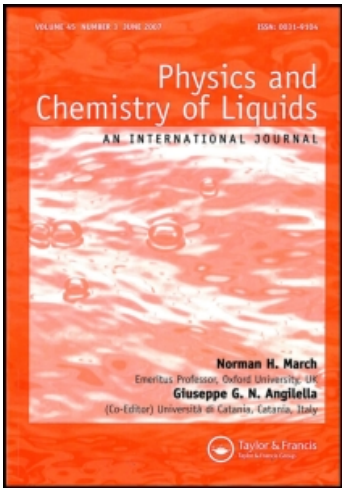

Physics and Chemistry of Liquids
Publication details, including instructions for authors and subscription information:
http://www.informaworld.com/smpp/title~content=t713646857

Neutron Diffraction Investigation of Liquid Li/Ba Alloys

H. Ruppersberg[a]
[a] Fachbereich Ingenieurwissenschaften, Universitat des Saarlandes, Saarbrucken, FRG

To cite this Article Ruppersberg, H.(1987) 'Neutron Diffraction Investigation of Liquid Li/Ba Alloys', Physics and Chemistry of Liquids, 17: 1, 73 — 89
To link to this Article: DOI: 10.1080/00319108708078542
URL: http://dx.doi.org/10.1080/00319108708078542

Phys. Chem. Liq., 1987, Vol. 17, pp. 73–89
Photocopying permitted by license only

Printed in the United Kingdom

Neutron Diffraction Investigation of Liquid Li/Ba Alloys

H. RUPPERSBERG

Fachbereich Ingenieurwissenschaften, Universität des Saarlandes, D-6600 Saarbrücken, FRG.

(Received 30 November 1986)

Liquid barium and liquid alloys of the ^{7}Li isotope with 12, 30 and 59 at% Ba were investigated by neutron diffraction in order to get information on the structure of simple liquid binary alloys of which the components differ strongly in size. Using pure liquid Li and Ba as a reference, the structure data of the alloys may quite well be approximated by hard-sphere curves. Significant deviation from hard-sphere behaviour is observed for intermediate distances in *r*-space and for the long wavelength concentration fluctuations. The value observed for the latter indicate a positive interchange energy for lithium rich alloys.

Key words: Neutron diffraction, liquid Li/Ba alloys, hard-sphere curves, *r*-space.

1 INTRODUCTION

In most liquid metals and alloys there is no direct covalent bonding between the atoms, and the structure is compact and relatively simple. If all the atoms of such a simple alloy have the same size, then the structure is close to substitutional, which means that the overall arrangement of the atoms is similar to the structure of a pure simple liquid metal with superimposed chemical short-range order[1]. For liquid alloys of this type and which have negative interchange energies, relations between structure, electronic properties and thermodynamic behaviour have been revealed recently by Hafner *et al.*[2] and by Ruppersberg and Schirmacher[3]. The situation is more complicated in the case of significant size difference between the components. Much work has been done to find a theoretical interpretation of thermodynamic properties and structural parameter of liquid Cs/Na alloys[4–12]. The ratios of the molar volumes and of the Fermi wave numbers of the pure components are 3 and 0.68, respectively. Model expressions for

ΔG, the Gibbs free energy of mixing, were based on the Flory–Huggins formula and hard-sphere equations, respectively. A formalism with similar significance to the one proposed by Hafner *et al.*[2] was however not found. We think that a broader experimental basis might be helpful and we hope that structure data which give a better insight into the distance correlation of concentration fluctuations will yield information of similar importance as in the case of substitutional alloys. We therefore started a program to investigate neutron diffraction pattern, density ρ, compressibility χ_T, specific heat C_p and surface tension Γ of Li alloyed with Ba, Sr and Ca. The ratios of the molar volumes of the pure components taken at their melting temperature T_L are 3.06, 2.61 and 2.19, respectively. Because the larger atoms are bivalent, the ratios of the radii of the Fermi sphere are much closer to unity than for Cs/Na. They amount to 0.86, 0.91 and 0.97 for Ba, Sr, Ca/Li, respectively; each radius taken at T_L. Little is known about other properties of these alloys and even the phase diagrams do not seem fully settled. The structure data obtained for ^{7}Li/Ba are discussed in this paper. ρ, C_p, χ_T and Γ of Li/Ba are given in a separate paper by Saar and Ruppersberg[13].

2 FORMALISM

2.1 Structure factor and Flory–Huggins equation

The diffraction experiments yield the total coherent scattering per atom, $I(q)$ with $q = 4\pi \sin\theta/\lambda$, where λ is the wavelength and θ is the scattering angle. We define the total structure factor by $S(q) = I(q)/\langle b^2\rangle$. For binary alloys consisting of N_i and N_j atoms of type i and j, respectively $(i, j = 1, 2)$ we have $\langle b^2\rangle = c_1 b_1^2 + c_2 b_2^2$ with $c_i = N_i/(N_1 + N_2)$. b_i is the coherent scattering length (of neutrons in the present case). $S(q)$ may be subdivided into three partial structure factors a_{ij} (Faber and Ziman[14]) related to the distance-correlation of particle–particle fluctuations or into the S_{mn} partial structure factors $(m, n = N, C)$ defined by Bhatia and Thornton[15] which refer to number (N) and concentration (C) fluctuations:

$$\begin{aligned} S(q) &= 1 + \{c_1^2 b_1^2 (a_{11}(q) - 1) + c_2^2 b_2^2 (a_{22}(q) - 1) \\ &\quad + 2c_1 c_2 b_1 b_2 (a_{12}(q) - 1)\}/\langle b^2\rangle \\ &= A_1 a_{11}(q) + B_1 a_{22}(q) + C_1 a_{12}(q) + c_1 c_2 \Delta b^2/\langle b^2\rangle \qquad (1) \end{aligned}$$

$$\begin{aligned} S(q) &= \{\langle b\rangle^2 S_{NN}(q) + 2\Delta b\langle b\rangle S_{NC}(q) + \Delta b^2 S_{CC}(q)/c_1 c_2\}/\langle b^2\rangle \\ &= A_2 S_{NN}(q) + B_2 S_{NC}(q) + C_2 \frac{S_{CC}(q)}{c_1 c_2} \qquad (2) \end{aligned}$$

b of the ^{7}Li isotope is negative which in our case makes C_1 negative and strongly increases the contrast of the $S_{CC}(q)$ term[1]. In fact, $\langle b \rangle = 0$ at the composition $Li_{70}Ba_{30}$ yielding $S(q) = S_{CC}(q)/c_1c_2$.

The long wavelength limit $S(0)$ of the total structure factor is related to the mean squared number density fluctuations $\langle \Delta N^2 \rangle = N \cdot S_{NN}(0)$, to the corresponding concentration fluctuations $\langle \Delta c^2 \rangle = S_{CC}(0)/N$, and to the cross term $S_{NC}(0) = \langle \Delta N \cdot \Delta C \rangle$. These fluctuations may be expressed in terms of the mean particle density ρ_0, the density ρ, the isothermal compressibility χ_T, the partial molar volumes v_i and the stability function $(\partial^2 \Delta G/\partial c^2)_{TPN} = Nk_BT/S_{CC}(0)$:

$$S(0) = \{\langle b \rangle^2 \rho_0 \cdot k_B T \chi_T + S_{CC}(0)[\langle b \rangle \cdot \rho(v_1 - v_2) - \Delta b]^2\}/\langle b^2 \rangle \quad (3)$$

k_B and T are the Boltzmann constant and the temperature, respectively. $S_{CC}(0)$ may thus be calculated from $S(0)$ if the other terms in Eq. (3) are known, which is the case for Li/Ba.

The Flory–Huggins equation relates ΔG to the molar volumes of the pure components V_i^0 and to the interchange energy ω, the latter was originally assumed to be independent of concentration and temperature. A q-dependent $\omega(q)$ corresponds in simple cases to the Fourier transform of the ordering potential (Ruppersberg and Schirmacher[3])

$$\Delta G = RT(c_1 \ln \phi_1 + c_2 \ln \phi_2) + \omega c_1 \phi_2 \quad (4)$$

The larger atoms are labelled "2" and $\phi_i = c_i V_i^0/(c_1 V_1^0 + c_2 V_2^0)$. Bhatia and March[16] derived from Eq. (4):

$$S_{CC}(0) = c_1c_2/\left\{1 + \frac{c_1c_2}{(c_1\beta + c_2)^2}\left[(1-\beta)^2 - \frac{2\omega}{RT}\frac{\beta}{(c_1\beta + c_2)}\right]\right\} \quad (5)$$

with $\beta = V_1^0/V_2^0$. Since for Li/Ba β is known, ω may be calculated from $S_{CC}(0)$. For ideal solutions $\beta = 1$ and $\omega = 0$, and S_{CC} becomes c_1c_2, which in this case is the value of $S_{CC}(q)$ for the whole q range. For athermal solutions $\omega = 0$, and (5) reduces to

$$S_{CC}(0) = c_1c_2/\{1 + c_1c_2 \cdot [(\beta - 1)/(c_1\beta + c_2)]^2\}, \quad (6)$$

$S_{CC}(0)$ is smaller than c_1c_2 and asymmetric about $c = 0.5$ (Bhatia[17]).

2.2 Information in *r*-space

Information in r-space is obtained from the Fourier transform of $S(q)$:

$$4\pi r^2(\bar{\rho}(r) - \rho_0) = \frac{2r}{\pi}\int q(S(q) - 1)\sin(qr) \cdot dq \quad (7)$$

which may again be expressed in terms of partial functions:

$$\begin{aligned} 4\pi r^2(\bar{\rho}(r) - \rho_0) &= 4\pi r^2\{c_1 b_1^2 \rho_{11}(r) + c_2 b_2^2 \rho_{22}(r) \\ &\quad + 2c_1 b_1 b_2 \rho_{12}(r) - \langle b\rangle^2 \rho_0\}/\langle b^2\rangle \\ &= 4\pi r^2\{A_8 \rho_{11}(r) + B_8 \rho_{22}(r) + C_8 \rho_{12}(r) \\ &\quad - \langle b\rangle^2 \rho_0/\langle b^2\rangle\} \end{aligned} \tag{8}$$

$\rho_{ij}(r)$ is the probability per unit volume of finding a j-particle at distance r from an i particle. Because of symmetry $c_1\rho_{12}(r) = c_2\rho_{21}(r)$. The $\rho_{ij}(r)$ are zero for distances r smaller than the closest possible approach between the particles and become $c_j\rho_0$ at large r. $Z_{ij} = \int_0^R 4\pi r^2 \rho_{ij}(r)\, dr$ gives the total number of j particles at a distance smaller than R from an i atom and corresponds to the coordination number if R is properly chosen. We insert for R the distance of the minimum of $4\pi r^2\rho_{ij}(r)$ following the first peak, or a value close to it, as explained later on in the text. At the composition $Li_{70}Ba_{30}$ $\langle b\rangle = 0$ and $4\pi r^2(\bar{\rho}(r) - \rho_0)$ calculated according to (7) gives directly the radial concentration correlation function RCF $= 4\pi r^2 \rho_{cc}(r)$ (Ruppersberg and Egger[18]).

2.3 Hard-Sphere formalism

The geometrical packing of atoms in a simple liquid is governed by the short range repulsive interactions and a system of random dense packed spheres (HS) presents a good starting point to calculate its structure and thermodynamic properties. Quantitative information about the structure of HS systems may be obtained from computer simulation studies and more easily by solving approximate analytical expressions of which the most useful is the Percus Yevick (PY) equation. It has been shown by Ashcroft and Lekner[19] that this equation allows to calculate $S_{HS}^{PY}(q)$ of monatomic systems as a function of the hard sphere diameter σ and the packing fraction η. Both are related by ρ_0:

$$\eta = \pi \cdot \rho_0 \cdot \sigma^3/6. \tag{9}$$

A better approximation for $S_{HS}(0)$ and thus for the compressibility is given by the Carnahan Starling[20] equation.

According to Young[21], $\rho_{HS}^{PY}(r)$ corresponds very well to results of computer simulation. This is demonstrated in Figure 1 where a $4\pi r^2(\rho_{HS}^{PY}(r) - \rho_0)$ curve is compared with the very precise Monte Carlo results of Barker and Henderson[22]. The spurious ripples close to $r/\sigma = 1$ are due to the finite integration length of $q_{max} = 270/\sigma$; they are suppressed in the figures which are shown later on in this paper.

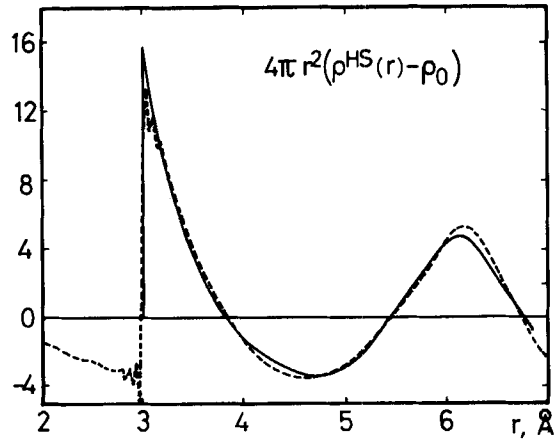

Figure 1 Hard-sphere $4\pi r^2(\rho(r) - \rho_0)$ curves, $\sigma = 3$ Å, $\eta = 0.47$. Full line: Monte Carlo results of Barker and Henderson[22]. Dashed line: From Percus Yevick structure factor, by integrating Eq. 7 with $q_{max} = 90$ Å^{-1}.

Liquid metals are evidently not really HS-systems and in reality $\rho(r)$ does not rise perpendicularly from zero in the way shown in Figure 1. That is why at large q the $S_{HS}(q)$ curves exhibit much stronger modulations and some phase shift in comparison with the experimental curves. The deviations are especially pronounced for the soft alkaline metals. Fitting the first peak of $S_{HS}^{PY}(q)$ to experimental curves yields empirical η (or σ) values which are tabulated for most liquid metals by Waseda[23] together with equations for their temperature variation.

It has been shown by Ashcroft and Langreth[24] that the PY-equation may also be solved for binary mixtures of hard spheres yielding partial structure factors $a_{ij}^{HS}(q)$; a corresponding computer program is given in Waseda's book[23]. The variables are the packing fraction $\eta = \eta_1 + \eta_2$ and the hard sphere diameters. Once again, these quantities are correlated

$$\eta = \pi \cdot \rho_0(c_1\sigma_1^3 + c_2\sigma_2^3)/6 \tag{10}$$

An extension of the Carnahan Starling equation proposed by Mansoori *et al.*[25] gives an expression for the free energy of mixing ΔF_{HS}:

$$\Delta F_{HS} = -T(\Delta S_{gas} + S_C + \Delta S_\eta + S_\sigma) = \Delta G_{HS}(\Delta V = 0) = -T\Delta S_{HS}^a \tag{11}$$

ΔS_{HS}^a corresponds to the entropy of mixing of an athermal HS-solution; ΔS_{gas} represents the ideal gas entropy, S_C is the ideal entropy of mixing. The terms ΔS_η and S_σ are the packing and misfit contributions to the entropy change respectively for which explicit formulae in terms of the

hard sphere diameters are available[9,26]. It has been observed by Visser *et al.*[9] and by Neale and Cusack[12] that the first term on the right side of Eq. (4) corresponds to $\Delta S_{\text{gas}} + S_C$ if ϕ_i is calculated with the real molar volume instead of $c_1 V_1^0 + c_2 V_2^0$.

Differentiation of the rather complex Eq. (11) (see Young[21]) yields $S_{CC}(0)$, which together with the Flory–Huggins formula (6) and the PY-equation is a third possibility to calculate this quantity for a binary noninteracting system of hard spheres.

2.4 Approaches for Na/Cs

It was mentioned in the introduction that much work has been done to find an interpretation of the properties of liquid Na/Cs in terms of the Flory–Huggins (FH) equation and the HS formalism, respectively; as well as in extensions and combinations of both methods. The heat of mixing is positive in this system (Yokokawa and Kleppa[4]), the activity coefficients are larger than one (Ichikawa *et al.*[5], Neale and Cusack[6]), and up to 6% volume contraction occurs on mixing (Huyben *et al.*[7]). ΔS is no more than 3% greater than that of an ideal solution and is independent of temperature. $S_{CC}(0)/c_1 c_2$, however, exhibits a pronounced maximum at about 75% Na with amplitude of 6.7 and 3.2 at 383 and 473 K, respectively (Huyben *et al.*[8]). The latter authors observed that for the interpretation of Na/Cs the FH formula suffers from quantitative inconsistencies. Visser *et al.*[9] used ΔS_{HS} for the entropy term in the FH equation but for an optimum reproduction of the experiments they had to admit a small composition dependence of the σ_i ($\leq 3\%$). $S_{CC}(0)$ came out to be very sensitive to the choice of σ_i. S_σ and ΔS_η were found to cancel each other almost exactly. Neale and Cusack[6] added a $p\Delta V$-term to Eq. (4) in order to take the volume contraction into account. Alblas *et al.*[10] tried to bring more consistency into the FH model by introducing a temperature dependent interchange energy, which originally was proposed by Bhatia *et al.*[27] and later on also used by Singh and Bhatia[11]. Neale and Cusack[12], finally, proposed an interacting HS model. They regarded ΔS_{HS} as well as ω as composition and temperature dependent parameters to be calculated by fitting to the experimental data. Coming from the caesium side, ω decreases by about 16%, remains almost constant between $0.2 < c_{\text{Cs}} < 0.7$ and rises by some percent at the sodium side; its temperature variation was only about half that observed by Alblas *et al.*[10] The composition variation of ΔS_{HS} is related to about 0.7% decrease of the σ_i values over the whole concentration range. The reason for the small excess entropy is seen to lie in the near cancellation of the contributions

arising from (a) the differing atomic volumes, and (b) the change in potential energy on mixing, the latter being much larger than the change of entropy of the free electron gas. The composition dependence of $S_{CC}(0)$ cannot be related to the molar volume difference and some form of longer ranged ion-ion interaction must be involved. The authors conclude that the latter completely dominates the departure from ideal behaviour in sodium rich alloys despite the fact that the sodium-caesium reaction is only moderately endothermic.

3 EXPERIMENTAL PROCEDURE

The samples were prepared inside a glove box containing high purity recycled argon. Starting material was 99.9% ^{7}Li and 99.5% Ba which originally contained 5 at% H. The hydrogen content could be reduced to about 1 at% by evacuating during several days a thin walled tantalum tube immersed into the liquid barium. The composition of the alloys was checked by chemical analysis. The liquid samples were poured into cylindrical container made from 0.1 mm vanadium foil with an external diameter of 11.4 mm and sealed by electron beam welding. The neutron diffraction experiments were carried out on the (old) D4 instrument of the Institut Laue Langevin, Grenoble, France, with experimental set-up and counting strategy as described by Ruppersberg and Reiter[28] who also give an outline of the data reduction. A severe problem was the correction for the scattering of hydrogen of which the concentration changed somewhat during sample preparation. For the Placzek correction we assumed the hydrogen to be dissolved as H-atoms and used a semi-empirical formula proposed by Chieux[29]. Because the absorption correction is quite sensitive to the H-content some iteration steps were necessary to find the H-content yielding the optimum structure factor. The total structure factors and the corresponding curves in r-space are given in Figures 3 to 6.

4 RESULTS

4.1 Pure Components

Figure 2 shows in the upper part as a full drawn line $S(q)$ of liquid Li measured at 595 K by neutron diffraction[30]. The dashed line is a HS-PY curve obtained by fitting to the position and amplitude of the first peak. This procedure yields excellent coincidence between experimental and PY-HS curve in r-space (lower part of Figure 2) at

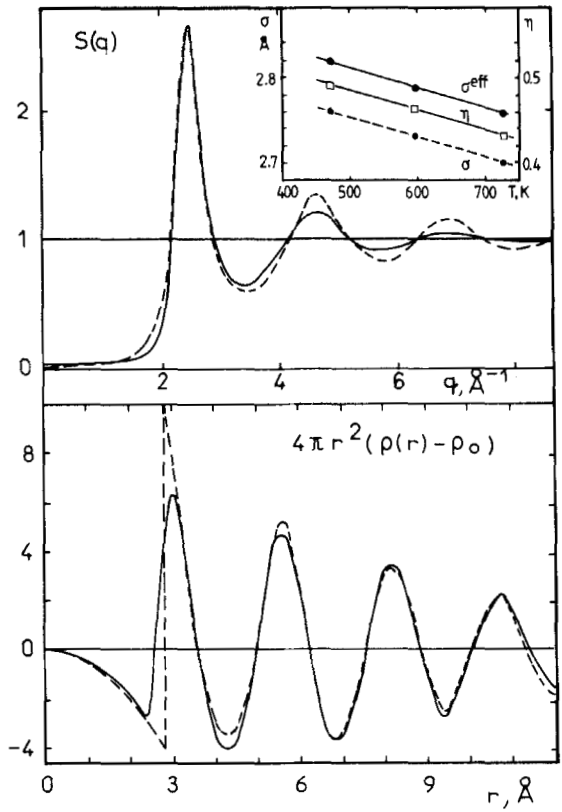

Figure 2 Structure factor (upper part) and $4\pi r^2(\rho(r) - \rho_0)$ curves (lower part) of liquid lithium at 595 K. Full lines: from neutron diffraction data. Dashed lines: PY-HS curves obtained from optimum fit to the first $S(q)$ peak, the HS parameter are given in Table 1. Insert: packing fraction η and effective HS-diameter σ^{eff} inserted into the PY equation to obtain the optimum fit at the given temperatures. σ calculated from η and ρ_0 according to Eq. 9 is drawn as a dashed line.

intermediate distances, which are the most interesting for the alloy curves. σ^{eff} and η obtained in this way are given in the inset of Figure 2 for 470, 595 and 725 K, respectively. From this plot one obtains $(d\eta/dT) = -2.3 \cdot 10^{-4}\,K^{-1}$ and $d\sigma/dT = -2.4 \cdot 10^{-4}\,Å \cdot K^{-1}$. Equation (9) yields $(d\rho_0/dT)/\rho_0 = -2.03 \cdot 10^{-4}\,K^{-1}$ which compares well to the value of $-2.13 \cdot 10^{-4}\,K^{-1}$ obtained from density measurements (Ruppersberg and Speicher[31]). σ calculated from η and ρ_0 using Eq. (9) is shown as a dashed line in Figure (2) and is seen to be 2% smaller than the "effective σ" from which the satisfactory $4\pi r^2(\rho(r) - \rho_0)$ curves were obtained.

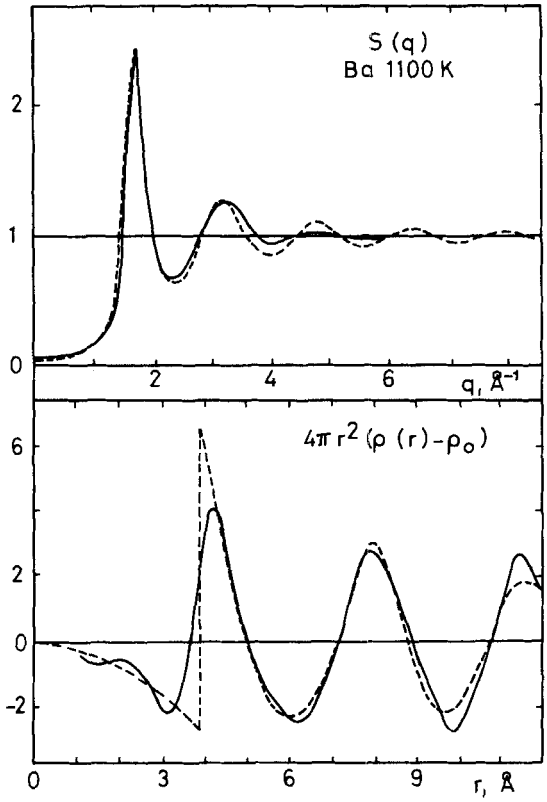

Figure 3 Structure factor (upper part) and $4\pi r^2(\rho(r) - \rho_0)$ curves (lower part) of liquid barium at 1100 K. Full lines: from neutron diffraction data. Dashed lines: PY-HS curves obtained from optimum fit to the first $S(q)$ peak. The HS parameters are given in Table 1.

An analogous procedure for liquid Ba yields the dashed HS-PY curves in Figure 3, calculated with $\eta = 0.44$ and $\sigma^{\text{eff}} = 3.95$ Å. The latter is once again about 2% larger than σ calculated from ρ_0 and η. Waseda[23] gives the following equation for the packing fraction of liquid Ba: $\eta(T) = 0.596 \exp(-2.84 \cdot 10^{-4}\, T)$ which yields $\eta(1100\,\text{K}) = 0.436$ in good agreement with our results. Inserting these values together with $(d\rho/dT)/\rho_0 = -0.9 \cdot 10^{-4}\,\text{K}^{-1}$ into the derivative with respect to T of Eq. (9) yields $d\sigma/dT = -2.55 \cdot 10^{-4}\,\text{Å} \cdot \text{K}^{-1}$.

The minima following the first peak of $4\pi r^2\rho(r)$ are at about 4 Å in both the experimental and the HS curve of liquid Li. The area which according to our definition corresponds to the coordination number is 12.1 and 11.5 atoms for the experimental and the HS curve, respectively.

The distances are 5.6 and 5.7 Å for liquid Ba, and the coordination numbers calculated for a distance of 5.65 Å amount to 11.6 and 11.0 atoms, again in the order of experimental and HS curve. For both Li and Ba the distance of the minimum is at about $1.43 \cdot \sigma$ and this value will be used for calculating the partial coordination numbers of the alloys as well, although the positions of the minima of the partial $4\pi r^2 \rho_{ij}(r)$ curves depend on concentration and are somewhat shifted with respect to the values of the pure components.

4.2 Structure data of the alloys

The σ_i values needed to calculate the PY-HS curves of the alloys were calculated from the σ_i^{eff} of the pure components and their temperature variations and are given in Table 1. η in the same table was calculated from η_i^0 of the pure components at the given temperature, assuming linear concentration dependence of the molar volume, which corresponds to the experimental observations[13]. η comes out to be linear if expressed as function of volume fraction: $\eta(\phi) = \eta_{\text{Li}}^0 + (\eta_{\text{Ba}}^0 - \eta_{\text{Li}}^0)\phi_{\text{Ba}}$, whereas $\eta(c)$ has a positive deviation from linear with a maximum relative amplitude of 3%. The contributions of the different partial structure factors to the total $S(q)$ according to Eqs (1) and (2) and of the partial radial distribution functions to $4\pi r^2(\bar{\rho}(r) - \rho_0)$ (Eq. (8)) are also summarized in Table 1.

Table 1 HS data and coefficients of the Eqs 1, 2 and 8 for the different liquids investigated.

Substance	T K	$\sigma_{\text{Li}}^{\text{eff}}$ Å	$\sigma_{\text{Ba}}^{\text{eff}}$ Å	η	Equation n	Coefficients		
						A_n	B_n	C_n
Li	595	2.79		0.462				
	575	2.795		0.465				
$Li_{88}Ba_{12}$	575	2.795	4.09	0.477	1	0.495	0.052	−0.322
					2	0.225	2.57	0.775
					8	0.559	0.433	−2.683
$Li_{70}Ba_{30}$	575	2.795	4.09	0.488	1	0.203	0.213	−0.416
					2	0	0	1
					8	0.290	0.710	−1.387
$Li_{41}Ba_{59}$	775	2.75	4.03	0.46	1	0.045	0.526	−0.306
					2	0.264	−1.793	0.736
					8	0.110	0.892	−0.519
Ba	575		4.09	0.506				
	1100		3.95	0.44				

$S(q)$ of the alloys is shown in the upper parts of the Figures 4 to 6. At small q, $S(q)$ is very different from $S_{HS}^{PY}(q)$ which will later be discussed in more detail. Beyond 1.5 $Å^{-1}$ the positions of the peaks are almost identical in the two sets of data. For the same reasons as for the pure components the amplitudes of the HS curves are much larger at high q. The curves in r-space show many more details. The modulations in the experimental curves at $r < 2.2$ Å are due to experimental errors and to failures in the data reduction. The HS curves are very helpful to discriminate between Li-Li, Ba-Ba and Li-Ba nearest neighbour distances, the latter giving a negative contribution. Besides the characteristic HS-steps, experimental and calculated curves are quite similar for distances up to about 6 Å and not totally different beyond this value where the deviations become more pronounced than for the pure

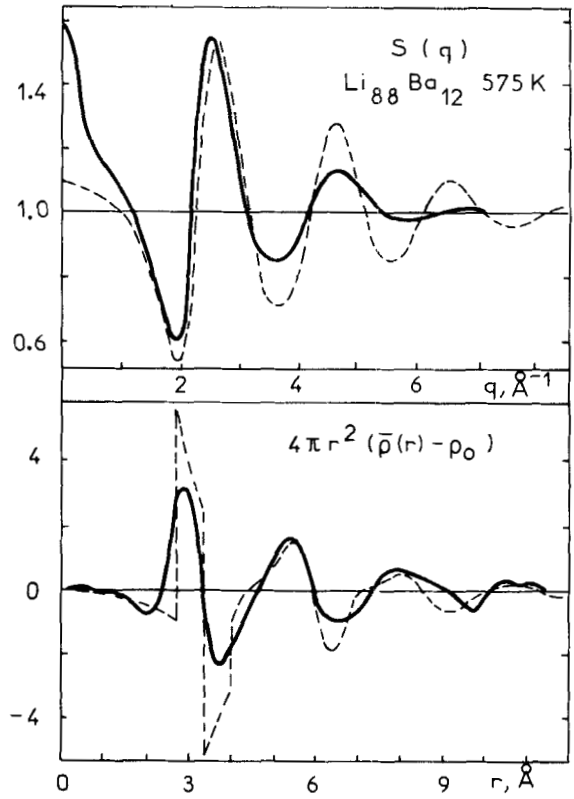

Figure 4 Total structure factor (upper part) and $4\pi r^2(\bar{\rho}(r) - \rho_0)$ curves (lower part) of liquid $Li_{88}Ba_{12}$ at 575 K. Full lines: from neutron diffraction data. Dashed lines: PY-HS curves calculated with parameter given in Table 1. Coefficients of the partial curves according to Eqs. 1, 2 and 8 are also given in Table 1.

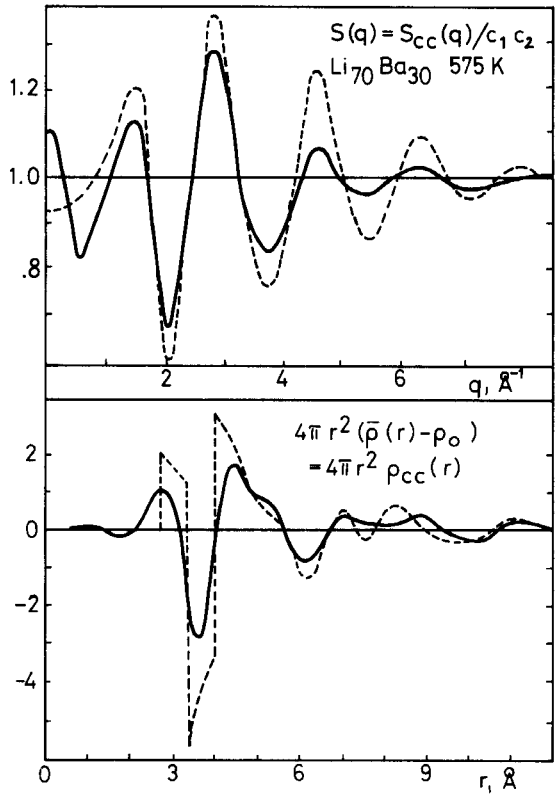

Figure 5 Structure data of liquid $Li_{70}Ba_{30}$ at 575 K, analogous to Figure 4.

components. Inspection of Figure 7 explains the origin of the shallow minimum at about 8 Å. It results from the second peaks of the partial curves which give a positive contribution for 1-1 and 2-2 distances but a negative one for 1-2 (see Table 1). It was not possible to obtain better agreement between experimental and calculated curves in the range between 6 and 9 Å, not even by varying η and the σ_i over a large scale. The observed irregularity is certainly not important for the thermodynamic properties, it indicates however that the structure as a whole deviates somewhat from that of a simple packing. More information can be obtained only by comparison with curves calculated on the basis of adequate interatomic potentials.

For substitutional alloys of non interacting equal size spheres, the coordination numbers Z_{ij} are proportional to c_j. The situation changes if the spheres differ in size. This is illustrated by the $4\pi r^2 \rho_{ij}(r)$ curves which are given in the upper part of Figure 7 for an equiatomic mixture.

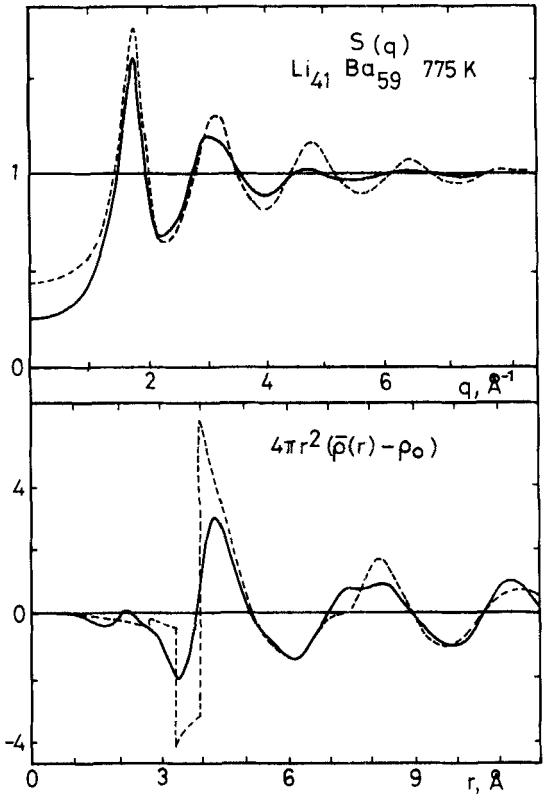

Figure 6 Structure data of liquid $Li_{41}Ba_{59}$ at 775 K, analogous to Figure 4.

Not only the coordination number but also the density at contact and the number of atoms for any distance interval in the region of the first peak is much smaller for the smaller species. Z_{ij}/c_j varies strongly with composition as is shown in the lower part of Figure 7. Z_{ij}/ϕ_j, however, is less affected, but its variation is still stronger than according to the increase in packing fraction on moving at constant temperature from the Li-side of the diagram to the Ba-side (see also Table 1). The total number of ij pairs is given by $N \cdot c_i \cdot Z_{ij} = N \cdot c_i(Z_{ij}/\phi_j) \cdot \phi_j$ and if Z_{ij}/ϕ_j is constant the number of pairs will vary with composition proportionally to $c_i\phi_j$, which is the basis of the interaction term of the Flory–Huggins equation.

4.3 $S_{cc}(0)$ of the alloys

$S_{CC}(0)/c_1c_2$ calculated from the athermal FH Eq. (6) and from the HS-Mansoori formalism based on Eq. (11) are shown in the upper part

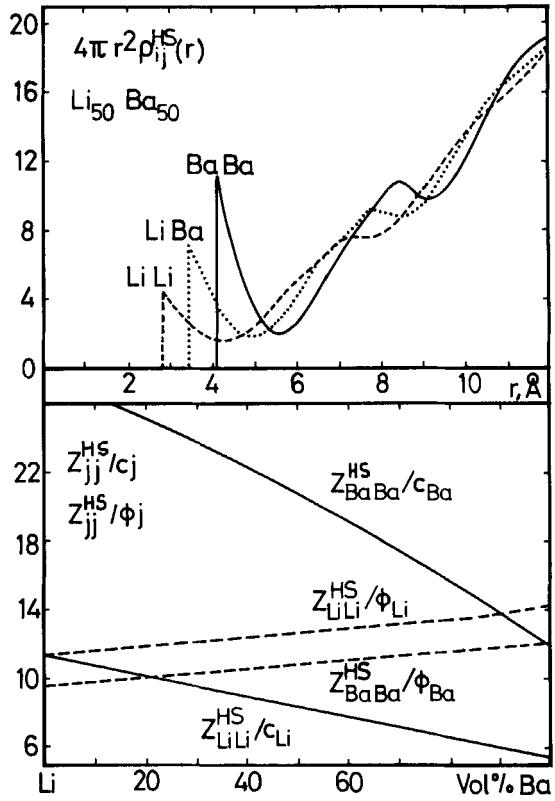

Figure 7 Upper part: Partial radial distribution functions of LiBa, calculated using the PY-HS formalism with $\sigma_{Li} = 2.795$, $\sigma_{Ba} = 4.09$ Å, and η calculated from η of the pure components at 575 K, given in Table 1 and assuming linear $V(c)$. Lower part: Relative partial coordination numbers as a function of volume fraction of Ba. c: atomic fraction, Φ: volume fraction.

of Figure 8. For the latter case two curves are given, assuming linear variation with composition of η and of V, respectively. Linear $V(c)$ is the more realistic description for Li/Ba. The deviations among the three curves are quite remarkable. It was mentioned above that $S_{cc}(0)$ in addition will strongly be affected by even a minor variation of σ_i with composition. Three points in this figure indicate the $S_{cc}(0)/c_1c_2$ values calculated from $S(0)$ according to Eq. (3). ω/RT calculated from Eq. (5) and the corresponding $\Delta H/R$ values are given in the lower part of Figure 8. The numerical values of ω/RT and of $\Delta H/R$ should not be taken too literally because they will come out different if based on one or the other HS equation instead of the FH free energy term. In addition it should be noted that $S(0)$ of $Li_{41}Ba_{59}$ was obtained at 775 K

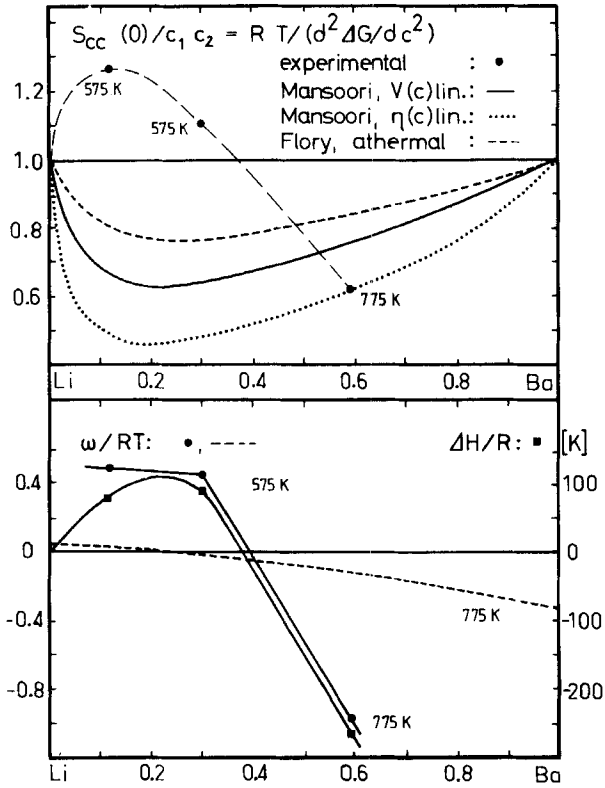

Figure 8 Upper part: $S_{cc}(0)/c_1c_2$. Points: from neutron diffraction data. Dashed line: From Flory-Huggins Eq. (5) assuming $\omega = 0$. Full curve: From Mansoori HS equation assuming linear $V(c)$. Dotted line: From Mansoori HS equation assuming linear $\eta(c)$. Lower part: Points: ω/RT (left hand scale) calculated from $S_{cc}(0)$ according to Eq. (5). Squares: $\Delta H/R$ (right hand scale) calculated from ω/RT. Dashed curve: ω/RT calculated from uniform background potential[32].

instead of 575 K for the other alloys. However, there is clear evidence for a positive deviation of $S_{cc}(0)/c_1c_2$ from the athermal mixture behaviour for lithium rich alloys, which may be related to a positive interchange energy.

Finally it should be noted that a refinement of the HS description of liquid metals and alloys is possible by introducing a negative structure independent uniform background potential u_g which gives rise to the cohesion of the real liquids. A simplifying formalism which is explained in detail in Shimoji's book[32] gives the energy of mixing as a sum of two terms: $\Delta E = \Delta E_{vc} + \Delta E_{ec}$. The first term is related to the changes on mixing of the kinetic energy of a free electron gas and of the energy of

placing the ions in the electron sea; its sign is positive. The second term, which is always negative or zero, comes from the charge transfer ΔZ between atoms of different kinds. ΔZ is obtained from $\partial u_g(V, \Delta Z)/\partial \Delta Z = 0$. The increase of the number of electrons on a Li site was found to vary from zero in pure Li to 0.33 in almost pure Ba. $\Delta E/R$ has a shallow maximum (about +4) at 10% Ba, changes sign at $c_{Ba} = 0.25$ and exhibits a minimum value (−35) at 70% Ba. ω/RT, defined according to Eq. 4, is shown as a dashed line in the lower part of Figure 8. The calculation was performed for a temperature of 775 K. However, here again the given numbers are of doubtful significance because the absolute values of ΔE_{vc} and ΔE_{ec} are about 100 and 10 times larger than ΔE at its maximum and minimum value, respectively, and $\Delta E(c)$ curves which are negative for all concentrations have been found for slightly varied packing fractions. In addition, an inclusion of the u_g term was not very helpful for a discussion of the physicochemical properties measured by Saar and Ruppersberg[13]. Application of more sophisticated theories seems premature until more thermodynamic data are available.

Acknowledgement

Financial help of the Deutsche Forschungsgemeinschaft and support from the Institut Laue Langevin (Grenoble, France) are gratefully acknowledged.

References

1. P. Chieux and H. Ruppersberg, *J. Physique Coll.*, **41**, C8, 145 (1980).
2. J. Hafner, A. Pasturel and P. Hicter, *J. Phys. F: Met. Phys.*, **14**, 1137 (1984); **14**, 2279 (1984); *Z. Metallkde.*, **76**, 432 (1985); *Phys. Rev.*, **B32**, 5009 (1985).
3. H. Ruppersberg and W. Schirmacher, *J. Phys. F: Met. Phys.*, **14**, 2787 (1984).
4. T. Yokokawa and O. Kleppa, *J. Chem. Phys.*, **40**, 46 (1964).
5. K. Ichikawa, S. M. Granstaff and J. C. Thomson, *J. Chem. Phys.*, **61**, 4059 (1974).
6. F. E. Neale and N. E. Cusack, *J. Phys. F: Met. Phys.*, **12**, 2839 (1982).
7. M. J. Huyben, K. Klaucke, J. Hennephof and W. van der Lugt, *Scr. Metall.*, **9**, 653 (1975).
8. M. J. Huyben, W. van der Lugt, W. A. M. Reimert, J. Th. M. de Hosson, and C. van Dijk, *Physica B & C*, **97**, 338 (1979).
9. E. G. Visser, W. van der Lugt and J. Th. M. de Hosson, *J. Phys. F: Met. Phys.*, **10**, 1681 (1980).
10. B. P. Alblas, J. Dijkstra, W. van der Lugt and A. B. Bhatia, *Phys. Chem. Liquids*, **12**, 255 (1983).
11. R. N. Singh and A. B. Bhatia, *J. Phys. F: Met. Phys.*, **14**, 2309 (1984).
12. F. E. Neale and N. E. Cusack, *J. Non Cryst. Solids*, **61&62**, 169 (1984); *Phys. Chem. Liquids*, **14**, 115 (1984).
13. J. Saar and H. Ruppersberg, *Phys. Chem. Liquids*, this volume.
14. T. E. Faber and J. M. Ziman, *Phil. Mag.*, **11**, 153 (1965).
15. A. B. Bhatia and D. E. Thornton, *Phys. Rev.*, **B2**, 3004 (1970).
16. A. B. Bhatia and N. H. March, *J. Phys. F: Met. Phys.*, **5**, 1100 (1975).

17. A. B. Bhatia, *Inst. Phys., Conf. Ser.*, **30**, 21 (1977).
18. H. Ruppersberg and H. Egger, *J. Chem. Phys.*, **63**, 4095 (1975).
19. N. W. Ashcroft and J. Lekner, *Phys. Rev.*, **145**, 83 (1966).
20. N. F. Carnahan and K. E. Starling, *J. Chem. Phys.*, **51**, 635 (1969).
21. W. H. Young, *Inst. Phys., Conf. Ser.*, **30**, 1 (1977).
22. J. A. Barker and D. Henderson, *Molecular Physics*, **21**, 187 (1971).
23. Y. Waseda, *The Structure of Non-Crystalline Materials*, McGraw Hill, New York (1980).
24. N. W. Ashcroft and D. C. Langreth, *Phys. Rev.*, **155**, 682 (1967); **159**, 500 (1967).
25. G. A. Mansoori, N. F. Carnahan, K. E. Starling and T. W. Leland, *J. Chem. Phys.*, **54**, 1523 (1971).
26. I. H. Umar, I. Yokoyama and W. H. Young, *Phil. Mag.*, **30**, 957 (1974).
27. A. B. Bhatia, N. H. March and L. Rivaud, *Phys. Lett.*, **47A**, 203 (1974).
28. H. Ruppersberg and H. Reiter, *J. Phys. F: Met. Phys.*, **12**, 1311 (1982).
29. P. Chieux, private communication.
30. H. Olbrich, H. Ruppersberg and S. Steeb, *Z. Naturforsch.*, **38a**, 1328 (1983).
31. H. Ruppersberg and W. Speicher, *Z. Naturforsch.*, **31a**, 47 (1976).
32. M. Shimoji, *Liquid Metals*, Academic Press, New York (1977), equation (205.6).